

# Big Data on the Fly: UAV-mounted Mobile Edge Computing for Disaster Management

Jianwen Xu, *Member, IEEE*, Kaoru Ota, *Member, IEEE*, and Mianxiong Dong, *Member, IEEE*

**Abstract**—After disasters, network communication is highly susceptible to disruption. In this case, we may need solutions without original architectures to meet the requirements of connectivity and communication. As a research hotspot, existing studies and practices in disaster management are often costly and may have to rely on differentiated strategies to deal with actual situations. In this paper, we choose UAVs as edge node carriers and LoRaWAN (Long Range Wide Area Networking) as a communication method in coping with mobile edge computing (MEC) for disaster management. Here we propose UAV-mounted MEC task management strategies to achieve emergency communication enabled by LoRaWAN. The system model includes two parts, air-to-ground and remote-to-air, in which we choose LoS/NLoS path loss model and log-distance to describe the connections. The experiment results show that our strategy can achieve low-cost, long-range MEC service, which can be quickly deployed in the affected area after disasters. We also choose path loss, SNR (signal-noise ratio), and channel capacity as performance metrics and prove that our solutions can increase the channel capacity while maintaining the same level of path loss and SNR.

**Index Terms**—Big Data Analytics, UAV Technology, Mobile Edge Computing, Disaster Management, Markov Chain.

## 1 INTRODUCTION

NATURAL disasters have been bringing enormous casualties and losses of property to us yearly. As one of the essential requirements in modern society, the communication network itself is extremely vulnerable to strong vibrations or flooding. Even large-area communication failure may occur when backbone base stations encounter issues such as power outage. Depending on the severity of disasters, it may take a long time for the original architecture to recover fully. Therefore, how to set up a fast-built network and manage the big data generated in emergency communication can be a problem to be settled urgently.

Existing studies in post-disaster networking and emergency communication mainly focus on how to increase the robustness of network structures and expand the scope of wireless signals, etc. However, similar practices may be costly on implementation, and strategies, as well as schemes, also have to consider a variety of actual situations, including network topology, user density, and device configuration. As a result, our target is to propose some approaches with high applicability and can be quickly deployed. Moreover, we also need countermeasures to cope with the failure of the original network infrastructure.

First, in the face of rapid deployment and high applicability, we choose UAVs as carriers to provide mobile edge services to users in affected areas. Unmanned aerial vehicle (UAV), or we used to call it a drone, refers to an aircraft without a pilot. UAV technology has been a new research hotspot in many areas and disciplines after rapid development in the past decade. The relatively low cost and flexible mobility instantly activate the internal potential of civilian UAVs. Especially for wireless communication and other fields, it offers many possibilities and scalability of

turning the ideas that used to exist only in the concept stage into reality. The leader of UAV manufacturing, DJI [1], has provided a complete set of solutions for multiple disciplines and fields such as agriculture, energy, public safety, construction, and infrastructure. And mobile edge computing (MEC), created by the European Telecommunications Standards Institute (ETSI) [2] with computing capacities and services implemented at the edge of the networks. MEC's decentralization attribute may enrich the structure of network topology that edge nodes can be deployed according to actual needs in disaster scenarios. As a result, with the help of UAV-mounted MEC, we can achieve fast networking [3] regardless of the topographic factors such as mountains or damaged roads.

Second, after finding the suitable service and its carrier, there remains the issue of how to establish connections in the disaster environment. That is, for emergency communication, we prefer low-cost, long-range transmission methods in the case of resource shortage, including electrical energy. To settle this issue, we choose LoRaWAN (Long Range Wide Area Networking) as our solution [4]. Working on the license-free radio frequency from 433 MHz (Europe), 915 MHz (North America) to 923 MHz (Asia), LoRa enables long-distance wireless connection up to 10 km with ultra-low power consumption [5]. As the IoT-oriented lightweight communication architecture other than the QoS awareness next-generation communication system, LoRa can just undertake the connection job between UAV-mounted mobile edge nodes and the remote control center.

A schematic of UAV-mounted MEC using LoRaWAN is shown in Fig. 1. Here we use a coordinate scale in the front to indicate the wireless communication range among user devices in the affected area, mobile edge nodes, and LoRa gateways. Here we make full use of the high mobility and unconstrained features of the UAVs and apply LoRa's long-distance low-power transmission in sending control

• Jianwen Xu, Kaoru Ota and Mianxiong Dong are with the Department of Sciences and Informatics, Muroran Institute of Technology, Japan.

Manuscript received November XX, 2019; revised XX XX, XXXX.

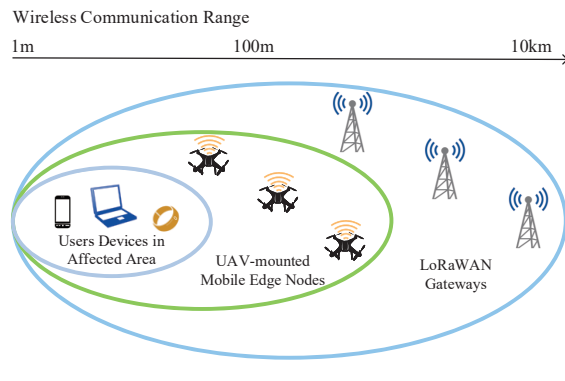


Fig. 1. A schematic of UAV-mounted MEC using LoRaWAN.

information to achieve fast networking and emergency communication. In our vision, the UAV-mounted MEC using LoRaWAN (UML) system can realize the big data on the fly, that is, collecting and processing data in the air by means of aerial vehicles and long-distance transmission to offer new technical support for disaster management.

We focus on the issue of task management in the UML system. That is, according to the demands from users trapped in disaster areas without any network signals, we set rules in offloading the computation resources in UAV-mounted mobile edge nodes. LoRaWAN here plays the role of connecting UAV nodes and the control center. The contributions are as follows.

- 1) We present a system model including three tiers: User Tier, UAV-mounted edge nodes as Service Tier, and LoRa concentrator & central server as Control Tier.
- 2) We model the UML system by two parts, air-to-ground between User Tier and Service tier, remote-to-air between Service Tier and Control Tier. We choose the LoS/NLoS path loss model and log-distance to describe the connections in two parts.
- 3) We apply the Markov chain to model the work state for each UAV node and the central server and propose two algorithms in settling task assignment and queue management.
- 4) We choose time and energy cost, path loss, SNR, and channel capacity as metrics in performance evaluation and consider different lengths of time-slot as well as user density. The results show that the strategies can help achieve low-cost, long-range MEC services in disaster management based on UAV and LoRaWAN.

Section 2 introduces the related researches about UAV technology in disaster management, MEC, and LoRaWAN. Section 3 builds the mathematical model and formulates the issues to cope with. Section 4 presents two algorithms in solving task assignment and queue management. Section 5 gives results of performance evaluation in consideration of different user densities and lengths of time-slot. Section 6 concludes our work.

## 2 RELATED WORK

Here we introduce the related work on the UAV technology in disaster management, mobile edge computing, and LoRaWAN.

### 2.1 UAV Technology in Disaster Management

Research on UAV technology has just begun to spring up after civilian UAV reaching the stage of industrialization. UAV does bring an unprecedented new possibility for the upcoming fourth industrial revolution. Mozaffari *et al.* focused on the D2D (device-to-device) communications with UAV. They also carried out studies on UAV's performance issues when assisting in wireless networking, including hovering time as well as antenna array gain [6]. Motlagh *et al.* presented a MEC & UAV-based platform for providing the Internet of Things (IoT) services. They demonstrated the potential of UAV technology in wireless communication networks and solved the problem of computation offloading in video stream processing to achieve face recognition based crowd surveillance [7]. Dong *et al.* presented a protocol for clone detection in cyber-physical systems (CPS) [8]. Sekander *et al.* evaluated the practicability of applying multi-tier UAV cellular networking in 5G and beyond 5G (B5G) and obtained the results of the spectral efficiency of transmission in the designed terrestrial network model through simulation [9]. Al-Hourani *et al.* focused on the problems of path-loss terrestrial and aerial covering in a real-world suburban area. They collected the reference signal received power (RSRP) from Long-Term Evolution (LTE) signal as the metric to test the performance in different propagation distances [10]. Hu *et al.* settled the problem of limited bandwidth assignment in UAV-assisted cellular networks [11].

In all aspects of disaster management (prevention, preparedness, relief, and recovery [12]), UAVs play an essential role in taking work that is difficult for manpower to complete. Erdelj *et al.* surveyed about the state-of-the-art applications in UAVs and wireless sensor networks (WSNs) [13]. Ota *et al.* proposed a game theory model in crowdsensing applications to make sure that all participants can be satisfied [14]. Naqvi *et al.* tried to implement a UAV-aided resilient wireless network infrastructure with a cross-layer resource allocation strategy for multiple application scenarios, including IoT service and disaster relief [15].

### 2.2 Mobile Edge Computing and LoRaWAN

Mobile edge computing not only has many technical characteristics inherited from cloud computing but also puts forward new requirements for equipment requirements and related technologies. And resource allocation is very critical in affecting communication and service quality. Sardellitti *et al.* designed an MEC network system to let mobile users request radio resources with minimized energy consumption and latency. They focused on the non-convex problem of global optimization in computation offloading using a successive convex approximate method [16]. You *et al.* also focused on computation offloading in MEC while considering a multi-user dedicated offloading system [17]. Tao *et al.* dealt with the problem of performance guaranteeing in MEC by applying Karush-Kuhn-Tucker (KKT) conditions in

designing a task offloading scheme for minimizing bandwidth capacity and energy consumption [18]. In the cross-field of UAV and 5G, MEC also has many applied kinds of research. Jeong *et al.* proposed a mobile cloudlet to optimize the downlink and uplink of wireless communications in MEC. They regarded UAV as an essential component of the mobile relaying system while considering its constraints on battery energy and trajectory under latency [19]. Wu *et al.* combined information-centric networking (ICN) in achieving content awareness security fog services [20] [21]. Li *et al.* paid attention to applying software-defined networking (SDN) in helping design data forwarding protocol for next-generation radio access network [22] and deep reinforcement learning for mobile crowdsensing [23].

As a representative of long-range communication technologies, LoRaWAN can provide low-cost network connections to geo-distributed IoT devices in urban or rural areas. Researches on LoRa are mainly about the determination and comparison of the performance in different environments. Petajajarvi *et al.* evaluated the signal range and channel attenuation model of LoRaWAN using 868 MHz (Europe) and 14 dBm as transmission power [24]. Bor *et al.* studied the limitations of LoRa connections, including path loss and receiver sensitivity [25]. Rizzi *et al.* paid attention to the time-related performance of distributed IoT networks based on LoRaWAN [26]. Georgiou *et al.* put forward a novel protocol framework different from the existing cellular network architecture [27]. Adelantado *et al.* summarized the issues on LoRa network capacity and the use cases, including environment monitoring and applications in smart city [28].

### 3 PROBLEM FORMULATION

Here we design a UAV-mounted mobile edge network model using LoRaWAN and formulate the problems to solve. Table 1 summarizes all the notations.

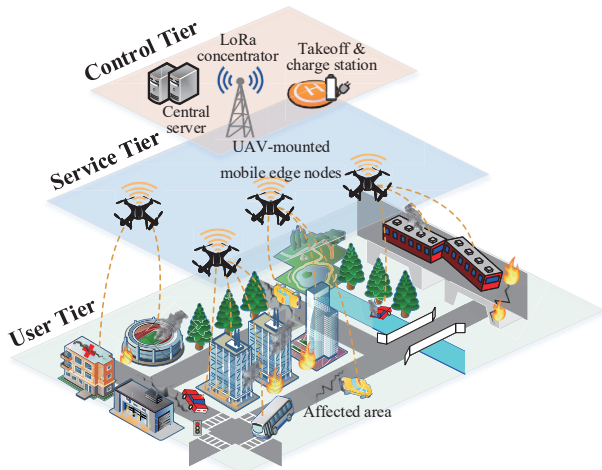


Fig. 2. UAV-mounted mobile edge computing network model using LoRaWAN.

In Fig. 2, we design a 3-tier network model using MEC and UAVs. First for User Tier, in an open area  $\mathbb{R}^2$  there are trapped users who follow spatial homogeneous Poisson point process [29]. Suppose the density of users is  $\rho_u$ , which

TABLE 1  
Notations

Notation	Description
$u_i, m_j$	User device and UAV node
$n_u, n_m$	Number of user devices, number of UAV nodes
$\rho_u$	Density of user devices in affected area
$\{\phi, \lambda, h\}$	GPS coordinates, latitude, longitude and height
$d_{i,j}, d_{j,s}$	Distances between $u_i, m_j$ and central server
$Pl^{los}, Pl^{nlos}$	Path losses of LoS and NLoS models
$Pl^{fs}, Pl^{ld}$	Path losses of free-space and log-distance models
$\gamma$	Path loss exponent
$X_g$	Gaussian random variable with zero-mean
$\theta$	Elevation angle
$\alpha, \beta$	Parameters in calculating probability of LoS and NLoS path losses
$SNR^{atg}, SNR^{rta}$	Signal-to-noise ratios of air-to-ground and remote-to-air parts
$b_m, b_c$	Bandwidths of UAV nodes and LoRa concentrator
$\sigma_g^2$	Power of Gaussian noise
$CC^{atg}, CC^{rta}$	Channel capacities of air-to-ground and remote-to-air parts
$t^{serv}$	Time cost on services provided by UML
$t^{ptl}, t^{fly}, t^{hov}$	Time cost on UAV patrolling, flying and hovering
$t_{ac}, t_{un}, t_{de}$	Flight time of acceleration, uniform speed and deceleration
$a_{ac}, a_{de}$	Acceleration and deceleration
$d_{ac}, d_{un}, d_{de}$	Fly distance of acceleration, uniform speed and deceleration
$v_p, v_{max}$	Speeds of patrol model and maximum
$t^{atg}, t^{rta}$	Time cost on air-to-ground and remote-to-air communications
$s_{pkt}$	Size of the packet being transmitted
$r_{bit}^{atg}, r_{bit}^{rta}$	Bit rates in air-to-ground and remote-to-air communications
$e^{serv}$	Energy consumption on services provided by UML
$e^{ptl}, e^{fly}, e^{hov}$	Energy consumption on UAV patrolling, flying and hovering
$g_0, m$	Gravitational acceleration and mass of UAV node
$\mu_1, \mu_2$	Parameters in helicopter aerodynamics
$a_c$	Centrifugal acceleration
$\tau, l_\tau$	Time-slot and length in Markov chain modeling
$x_i^m, x_i^s$	Task indicators of two tiers requested by $u_i$
$Q_t$	FIFO task queue in UML
$C_Q$	Capacity of $Q_t$
$\eta$	Number of new tasks being pushed into $Q_t$
$y^m, y^s$	Work state indicators of two tiers
$C_s$	Resource capacity in central server
$\xi^m, \xi^s$	Numbers of tasks solved by two tier
$SS$	State space of UML system
$\Pi, pr$	Stationary distribution and transition probability in time-homogeneous Markov chain

stands for the user number per unit area. As a result, the probability of  $n_u$  users existing in the unit area is

$$P(n_u) = \frac{\rho_u^{n_u}}{n_u!} e^{-\rho_u} \quad (1)$$

Then for Service Tier, to provide MEC services to User

Tier, we need UAVs as carriers to take edge devices, including Raspberry Pi, LoRa module, while patrolling above the affected area. When any UAV-mounted edge node  $m_j$  receives a request from user  $u_i$ , it will switch to fly mode and draw near the sender by GPS coordinates  $\{\phi, \lambda, h\}$ . In our model design, we focus on the horizontal flight of UAVs, and the  $h$  is mainly for calculation of path loss. As a result, the distance between the current UAV node and hover position suitable for rendering MEC service is

$$d_{i,j} = \sqrt{(\phi_i - \phi_j)^2 + (\lambda_i - \lambda_j)^2 + (h_i - h_j)^2} \quad (2)$$

where  $\{\phi_j, \lambda_j, h_j\}$  and  $\{\phi_i, \lambda_i, h_i\}$  are the GPS coordinates of UAV node  $m_j$  and user device  $u_i$ 's antennas.

Lastly, the top Control Tier, as shown in Fig. 2, there exists a central server, LoRaWAN gateway, and takeoff & charge station for UAVs. The central server includes the data storage needed by disaster relief and responds to uplink messages sent back by UAV nodes according to the proposed task management strategy. Gateways in LoRaWAN are also known as concentrators, which play the role of signal relay equipment to build connections between the server and end devices as LoRaWAN nodes. The takeoff & charge station is for UAVs.

### 3.1 System Model

#### 3.1.1 Air-to-ground part

After introducing the three tiers of the network model, first, we model the connection between Service Tier in the air and User Tier on the ground. There exist two path loss models in the case of the line-of-sight (LoS) and non-line-of-sight (NLoS) in the air-to-ground part [30].

$$Pl^{los}(d_{i,j}) = Pl^{fs}(d_{fs}) + 10\gamma_{los}\log_{10}d_{i,j} + X_g^{los} \quad (3)$$

$$Pl^{nlos}(d_{i,j}) = Pl^{fs}(d_{fs}) + 10\gamma_{nlos}\log_{10}d_{i,j} + X_g^{nlos} \quad (4)$$

Equations (3) and (4) show the results of LoS path loss and NLoS in in Decibel (dB), respectively.  $\gamma$  and  $X_g$  are path loss exponent and Gaussian random variable with zero-mean.  $d_{fs}$  is reference distance of free-space model.  $Pl^{fs}$  stands for the free-space path loss which is (in dB)

$$Pl^{fs}(d_{fs}) = 20\log_{10}\left(\frac{d_{fs}f4\pi}{c}\right) \\ = 20\log_{10}d_{fs} + 20\log_{10}f - 147.55 \quad (5)$$

where  $f$  stands for the frequency (Hz) and  $c$  as the speed of light, respectively.  $d_{fs}$  is the free-space reference distance. We have  $d \gg c/f$ , and both antennas are in the far-field of each other. Then according to the actual situation in which the occlusion may occur, we have the probability of LoS [31]

$$P^{los}(\theta) = \frac{1}{1 + \alpha e^{-\beta(\theta - \alpha)}} \quad (6)$$

where  $\alpha$  and  $\beta$  refer to the parameters of this Sigmoid function.  $\theta$  is the elevation angle calculated by

$$\theta = \sin^{-1}\left(\frac{|h_i - h_j|}{d_{i,j}}\right) \quad (7)$$

And the probability value of NLoS is

$$P^{nlos}(\theta) = 1 - P^{los}(\theta) \quad (8)$$

As a result, we have the path loss model of the first air-to-ground part

$$Pl^{atg}(d_{i,j}, \theta) = P^{los}(\theta)Pl^{los}(d_{i,j}) + P^{nlos}(\theta)Pl^{nlos}(d_{i,j}) \quad (9)$$

Using the result of path loss, then we obtain the signal-to-noise ratio (SNR)

$$SNR^{atg} = \frac{p_m^{tran}}{10^{0.1Pl^{atg}(d_{i,j}, \theta)} \cdot \sigma_g^2} \quad (10)$$

where  $p_m^{tran}$  is the transmission power of the UAV node.  $\sigma_g^2$  stands for the power of Gaussian noise. Lastly, we have the channel capacity between UAV node  $m_j$  and user device  $u_i$  which means the tight upper bound on the transmission rate (bits/s)

$$CC^{atg} = \frac{b_m}{n_u} \log_2(1 + SNR^{atg}) \quad (11)$$

As shown in Equation (11),  $b_m$  is the bandwidth of UAV node.

#### 3.1.2 Remote-to-air part

Second, we model the communication between LoRaWAN concentrator in Control Tier and UAV-mounted mobile edge nodes in Service Tier. Based on the LoRaWAN technology, we can build connections between the remote concentrator and UAV nodes. Different from the air-to-ground part, we choose the log-distance path loss model to figure out the path loss here [25].

$$Pl^{rta}(d_j) = Pl(d_0) + 10\gamma_{ld}\log_{10}(d_j/d_0) + X_g^{ld} \quad (12)$$

where  $d_j$  is the distance between UAV node  $m_j$  and LoRa concentrator.  $Pl(d_0)$  refers to the path loss at the reference distance  $d_0$ .  $\gamma_{ld}$  &  $X_g^{ld}$  respectively stands for path loss exponent and Gaussian random variable with zero-mean. The SNR of remote-to-air part is given by

$$SNR^{rta} = \frac{p_c^{tran}}{10^{0.1Pl^{rta}(d_j)} \cdot \sigma_g^2} \quad (13)$$

where  $p_c^{tran}$  stands for the transmission power of concentrator. And channel capacity between the concentrator and UAV node  $m_j$  is

$$CC^{rta} = \frac{b_c}{n_m} \log_2(1 + SNR^{rta}) \quad (14)$$

where  $b_c$  is the bandwidth of LoRa concentrator, and  $n_m$  is the number of UAV nodes.

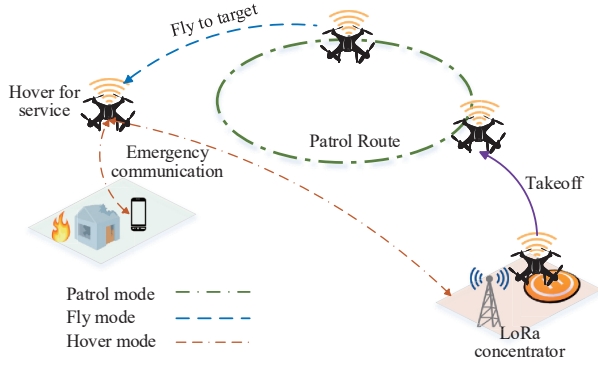


Fig. 3. A sketch of UAV-mounted MEC service mode

### 3.2 Performance Metrics

To achieve efficient task management in UAV-mounted mobile edge computing using LoRaWAN, we choose two main metrics, service time and energy consumption for performance evaluation.

First, to calculate service time, we consider three parts, that is, patrol time, flight time, and hover/transmission time.

$$t_{i,j}^{serv} = t_{i,j}^{ptl} + t_{i,j}^{fly} + t_{i,j}^{hov} \quad (15)$$

As shown in Fig. 3 and Equation (15), after taking off from ground station, UAV nodes first may switch to patrol mode. We regard this mode as a preparation phase that enables UAV nodes to surround the affected area according to the specified route within the signal coverage of the LoRaWAN concentrator. Patrol time  $t_{i,j}^{ptl}$  can be calculated by  $v_p$ .

When a  $m_j$  receives a request from the user device, it then may temporarily suspend the patrol mode and determine the hovering position based on the GPS information being uploaded. And to get close to the target as quickly as possible, UAV nodes need to speed up.

$$t_{i,j}^{fly} = t_{ac} + t_{un} + t_{de} \quad (16)$$

where  $t_{ac}$ ,  $t_{un}$ ,  $t_{de}$  respectively stands for the time cost on the process of acceleration, uniform speed and deceleration. In case the maximum speed  $v_{max}$  is reached, we have

$$\begin{aligned} d_{i,j} &= d_{ac} + d_{un} + d_{de} \\ &= v_p t_{ac} + \frac{1}{2} a_{ac} t_{ac}^2 + v_{max} t_{un} + \frac{1}{2} a_{de} t_{de}^2 \end{aligned} \quad (17)$$

where  $d_{ac}$ ,  $d_{un}$  and  $d_{de}$  are distances traveled during acceleration, uniform speed and deceleration, respectively.  $v_p$  is the patrol speed.  $a_{ac}$  and  $a_{de}$  are acceleration and deceleration values.

Last and most important, the time cost on inter-tier emergency communications. After switching to the hover mode, UAV nodes play the role of signal relay equipment. That is, sharing LoRa signals transmitted over long distances to user devices.

$$\begin{aligned} t_{hov} &= t_{atg} + t_{rta} \\ &= s_{pkt}/r_{bit}^{atg} + s_{pkt}/r_{bit}^{rta} + (d_{i,j} + d_{j,s})/c \end{aligned} \quad (18)$$

As shown in Equation (18), we calculate the transmission time cost on both two parts, air-to-ground and remote-to-air. Both parts need to consider transmission delay and propagation delay. For the former, the size of the packet to be transmitted  $s_{pkt}$  and data transmission rate  $r_{bit}$  are needed. For the latter,  $d_{i,j}$  &  $d_{j,s}$  (distances between  $u_i$ ,  $m_j$  and central server), and  $c$  (the speed of light) are needed.

According to the demand of users, sometimes we do not need help from Control Tier, the request can be answered by UAV nodes, such as uploading the injury report. In other cases, users may want to send messages to the outside world; thus, we have to consider  $t_{rta}$ .

Secondly, the energy consumption of UAV-mounted MEC using LoRaWAN in three modes. Here we focus on is the energy cost of UAV nodes; that is, the part provided by the UAV onboard batteries. Under current manufacturing technology, battery capacity is still one of the bottlenecks limiting the work performance of UAVs. As a result, in this paper, we are committed to maximizing the utilization of battery power when processing requests from User Tier with a suitable task management strategy.

$$e^{serv} = e^{ptl}(t_{i,j}^{ptl}) + e_{i,j}^{fly}(t_{i,j}^{fly}) + e^{hov}(t_{i,j}^{hov}) \quad (19)$$

Similar to time cost, we consider three parts of power consumption on UAV batteries.  $e_{i,j}^{fly}$  stands for the part on movement from the where  $m_j$  is to the hover position for  $u_i$ . The reason why we do not consider the part on transmission using LoRaWAN is that comparing with the cost of flying, transmission cost almost can be negligible. For example, DJI Matrice 100 as the UAV model for development can hover for 22 min with the standard 4500 mAh TB47D battery [1], and LoRa module RAK811 which can be embedded on UAV has the maximum transmit power of 20 dBm/100 mW [32].

$$\begin{aligned} e^{ptl+fly}(t_{i,j}^{ptl} + t_{i,j}^{fly}) \\ = \int_0^{t_{i,j}^{ptl}+t_{i,j}^{fly}} [\mu_1 v(t)^3 + \frac{\mu_2}{v(t)} (1 + \frac{a_c(t)^2}{g_0^2})] dt \\ + \frac{1}{2} m [v(t_{i,j}^{fly})^2 - v(0)^2] \end{aligned} \quad (20)$$

As shown in Fig. 20 [33] [34], according to some principles in helicopter aerodynamics, we use  $v(t)$  to indicate the speed which can be changed in acceleration and deceleration.  $g_0$  stands for the gravitational acceleration, and  $m$  refers to the mass of UAV node.  $\mu_1$  and  $\mu_2$  are two parameters given by

$$\begin{aligned} \mu_1 &= \frac{1}{2} \rho_{air} C_{D,0} A_p \\ \mu_2 &= \frac{2(mg_0)^2}{\pi e_0 r_{as} \rho_{air} A_p} \end{aligned} \quad (21)$$

where  $\rho_{air}$  stands for the air density, and  $C_{D,0}$  is the zero-lift drag coefficient, which relates to UAV's size, speed, and flying altitude.  $A_p$  is the area of the propellers on UAV,  $r_{as}$  is the aspect ratio of propellers.



Since the procedure of  $e_{i,j}^{fly}$  is switched from patrol mode and ending at hover mode while fly speed drops to zero. As a result, the right half of Equation (20) can be

$$\frac{1}{2}m[v(t_{i,j}^{fly})^2 - v(0)^2] = \frac{1}{2}m[0^2 - v_p^2] = -\frac{1}{2}mv_p^2 \quad (22)$$

Besides,  $a_c$  in Equation (20) means the centrifugal acceleration, which refers to an inertial force directed away from the axis of rotation.

$$a_c(t) = \sqrt{\mathbf{a}(t)^2 - \frac{(\mathbf{a}^T(t)\mathbf{v}(t))^2}{\mathbf{v}(t)^2}} \quad (23)$$

where  $\mathbf{a}^T$  and  $\mathbf{v}$  are acceleration and speed in vector form, respectively. Energy consumption on UAV hovering is given by [35]

$$e^{hov}(t) = e^{atg} + e^{rta} = p^{hov}(t^{atg} + t^{atg}) \quad (24)$$

### 3.3 Markov Chain Modeling

After modeling the UAV flying and metrics for performance evaluation, in this subsection, we present a time-homogeneous Markov chain for modeling the procedure of task management. First, we define a task queue  $Q_t$  to collect in the central server all the requests from user devices, which are forwarded by UAV nodes through LoRa connections. And for the process of the task at the head of  $Q_t$ , we denote it as one time-slot. That is, in the current  $\tau$ , our target is to handle the task of the queue header. Then for  $\tau$ , there exist two results that the current task can be finished by UAV nodes in Service Tier or by the central server in Control Tier [36].

$$x_i^m(\tau), x_i^s(\tau) \in \{0, 1\} \quad (25)$$

Equation (25) shows the results in time-slot  $\tau$ .  $x_i^m(\tau) = 1$  means the  $u_i$  is asking for service from UAV nodes, and  $x_i^m(\tau) = 0$  means not, the same with  $x_i^s(\tau)$  of central server. That is,  $\{x_i^m(\tau), x_i^s(\tau)\} = \{1, 1\}$  stands for the case that  $u_i$  asks for help from either of the two tiers. And  $\{x_i^m(\tau), x_i^s(\tau)\} = \{0, 0\}$  is for the case that  $u_i$  does not send request. We use an FIFO (First In First Out)  $Q_t(\tau)$  to display the number of requests still not finished in  $\tau$ . As a result, in  $\tau + 1$  we have

$$Q_t(\tau+1) = \begin{cases} Q_t(\tau) - f(\tau) + \eta(\tau), & \text{if } Q_t(\tau) + \eta(\tau) \leq C_Q \\ C_Q - f(\tau), & \text{if } Q_t(\tau) + \eta(\tau) > C_Q \end{cases} \quad (26)$$

where  $C_Q$  stands for the maximum capacity of the queue. In our design, UAV nodes can collect user requests and upload to LoRa concentrator no matter they are patrolling, flying, or hovering for service. And  $\eta(\tau)$  stands for the number of new tasks being pushed into  $Q_t$  within this  $\tau$ .  $f(\tau)$  is a function given by

$$f(\tau) = \sum_{i=1}^{n_u} f_i(\tau) = \frac{1}{2} \sum_{i=1}^{n_u} [x_i^m(\tau) + x_i^s(\tau) + |x_i^m(\tau) - x_i^s(\tau)|] \quad (27)$$

Equation (27) gives the results of requests sent by all  $n_u$  user devices in  $\tau$ . In the case that task needs the help of

both tiers  $\{x^m(\tau), x^s(\tau)\} = \{1, 1\}$ , we expect the output to be no more than 1. Next, we determine the work state of the Service Tier and the Control Tier.

$$y^m(\tau), y^s(\tau) \in Z, 0 \leq y^m(\tau) \leq n_m, 0 \leq y^s(\tau) \leq C_s \quad (28)$$

Similar with Equation (25), numerical values in Equation (28) stand for the number of tasks occupying this tier, 0 stands for idle state. For Service Tier, each UAV node can only serve for one user device, that is  $y^m(\tau) = n_m$  means all  $n_m$  UAV nodes are busy. As a result, for the hovering position, we consider that it is an ideal choice to let UAVs hover directly above the users. Then, for Control Tier,  $y^s(\tau) = C_s$  means the central server is reaching the capacity of computational resource in  $\tau$ .

$$y^m(\tau+1) = \begin{cases} y^m(\tau) + \sum_{i=1}^{n_u} x_i^m(\tau) - \xi^m(\tau), & \text{if } y^m(\tau) + \sum_{i=1}^{n_u} x_i^m(\tau) \leq n_m \\ n_m - \xi^m(\tau), & \text{if } y^m(\tau) + \sum_{i=1}^{n_u} x_i^m(\tau) > n_m \end{cases} \quad (29)$$

$$y^s(\tau+1) = \begin{cases} y^s(\tau) + \sum_{i=1}^{n_u} x_i^s(\tau) - \xi^s(\tau), & \text{if } y^s(\tau) + \sum_{i=1}^{n_u} x_i^s(\tau) \leq C_s \\ C_s - \xi^s(\tau), & \text{if } y^s(\tau) + \sum_{i=1}^{n_u} x_i^s(\tau) > C_s \end{cases} \quad (30)$$

As shown in Equations (29) and (30), in the next time-slot  $\tau + 1$ ,  $x_i^m(\tau)$  and  $x_i^s(\tau)$  newly come into the processing unit of two tiers.  $\xi(\tau)$  stands for the number of tasks finishing. Here we use  $SS$  to denote the state space of the UML system in Markov chain.

$$SS(\tau) = \{Q_t(\tau), y^m(\tau), y^s(\tau)\} \quad (31)$$

As a result, the discrete state space is finite and can be shown as a three-dimensional matrix with  $C_Q$  by  $n_m$  by  $C_s$ .

### 3.4 Problem Formulation

First, according to Equations (15) and (18), the problem on service time in total is given by

$$\sum_{\tau} t_{\tau}^{serv} = \sum_{\tau} \sum_{i=1}^{n_u} [P_{1,0}^x(\tau)(t^{atg,i} + t_i^{ptl} + t_i^{fly}) + (P_{0,1}^x(\tau) + P_{1,1}^x(\tau))(t^{atg,i} + t^{rta,i} + t_i^{ptl} + t_i^{fly})] \quad (32)$$

where  $t_{\tau}^{serv}$  denotes the service time generated in  $\tau$ .  $P_{0,0}^x(\tau)$ ,  $P_{0,1}^x(\tau)$ ,  $P_{1,0}^x(\tau)$  and  $P_{1,1}^x(\tau)$  are probabilities of four cases in Equation (25). That is, within this time-slot, some of requests/tasks sent by user devices in front of the  $Q_t$  get answered. The ones on Control Tier enter the processing unit of central server, and the ones on Service Tier are being allocated to the UAV nodes nearby. Thus, together with Equation (1), our target of reducing time cost in UML system is

$$\begin{aligned}
& \text{minimize} \quad P(n_u) \sum_{\tau} t_{\tau}^{serv} \\
& \text{subject to} \quad C1: P_{0,0}^x(\tau) + P_{0,1}^x(\tau) + P_{1,0}^x(\tau) + P_{1,1}^x(\tau) = 1 \\
& \quad C2: 0 \leq \Pi_i \leq 1, \sum_{i \in SS} \Pi_i = 1, \Pi_i = \sum_{j \in SS} \Pi_j pr_{i,j}
\end{aligned} \quad (33)$$

C2 in (33) is the steady-state condition in time-homogeneous Markov chain [37].  $\Pi$  stands for the stationary distribution and  $pr_{i,j}$  is the transition probability from  $\Pi_j$  to  $\Pi_i$ .

Second, according to Equation (20), the problem of energy cost on UAV batteries is given by

$$\begin{aligned}
\sum_{\tau} e_{\tau}^{ptl+fly} &= \sum_{\tau} \sum_{i=1}^{n_u} \left\{ \int_0^{t_i^{ptl}+t_i^{fly}} [\mu_1 v(t)^3 + \frac{\mu_2}{v(t)} (1 + \frac{a_c(t)^2}{g_0^2})] dt \right. \\
&\quad \left. + \frac{1}{2} m [v(t_i^{ptl} + t_i^{fly} + \tau l_{\tau})^2 - v(\tau l_{\tau})^2] \right\}
\end{aligned} \quad (34)$$

where  $l$  stands for the length of a single time-slot, that is, we calculate the part energy consumption from the end of the current  $\tau$  to arrival at hover position.

$$\begin{aligned}
\sum_{\tau} e_{\tau}^{hov} &= p^{hov} \sum_{\tau} \sum_{i=1}^{n_u} \{ P_{1,0}^{x_i}(\tau) t^{atg,i} \\
&\quad + [P_{0,1}^{x_i}(\tau) + P_{1,1}^{x_i}(\tau)] (t^{atg,i} + t^{rta,i}) \}
\end{aligned} \quad (35)$$

Similarly, together with Equations (1) and (19), our target of reducing energy consumption in UML system is

$$\begin{aligned}
& \text{minimize} \quad P(n_u) \sum_{\tau} (e_{\tau}^{ptl+fly} + e_{\tau}^{hov}) \\
& \text{subject to} \quad C1: P_{0,0}^x(\tau) + P_{0,1}^x(\tau) + P_{1,0}^x(\tau) + P_{1,1}^x(\tau) = 1 \\
& \quad C2: 0 \leq \Pi_i \leq 1, \sum_{i \in SS} \Pi_i = 1, \Pi_i = \sum_{j \in SS} \Pi_j pr_{i,j}
\end{aligned} \quad (36)$$

In consideration of the uncertainty in calculating different parts in Equations (33) and (36), there may even exist difference in order of magnitude. As a result, in the design of task management strategies, we focus on taking care of each part from a global perspective and looking for multi-objective solutions.

#### 4 TASK MANAGEMENT STRATEGY FOR UAV-MOUNTED MEC USING LoRAWAN

In this section, we design task management strategies for UAV-mounted MEC service using LoRaWAN in a post-disaster scenario.

To solve the two problems shown in (33) and (36), we design two algorithms in handling task assignment and task queue management during the operation of the UML system. First, we propose an algorithm for allocating the tasks collected by the LoRa concentrator to UAV nodes in Service Tier. The tasks being offloaded to UAV are unified as file transfer. That is, users are requesting for files (such as rescue guide, evacuation map, etc.) with different sizes and

UAVs are building the bridges between affected areas and the outside world. Here the central server plays the role of a backup service provider to take over the tasks in need of high computational resource consumption.

#### Algorithm 1 STAS: Single Task Assignment Strategy

---

```

1: this_task // the current task from  $u_i$ 
2:  $d_{min}^*$  // the shortest distance between  $u_i$  and any idle  $m_j$ 
3:  $\{x^m(\tau), x^s(\tau)\}$  // the results whether the task can be assigned
   to Server Tier and Control Tier
4: loop
5:    $\tau = \tau + 1$ 
6:   this_task( from  $u_i$ )  $\leftarrow Q_t.pop()$ 
7:   if this_task. $x^m(\tau) = 1$  || this_task. $x^s(\tau) = 1$  then
8:     if find( $m_j | m_j.state = 0 \ \&\& \ dist(m_j, u_i) = d_{min}^*$ )
       then
9:       if this_task. $x^m(\tau) = 1$  then
10:         $m_j.state \leftarrow 0$ , this_task. $x^m(\tau) \leftarrow 0$ ,
11:        this_task. $x^s(\tau) \leftarrow 0$ 
12:       else if  $C_s < C_{max}$  then
13:         $C_s \leftarrow C_s + 1$ , this_task. $x^s(\tau) \leftarrow 0$ 
14:       end if
15:     end if
16:   end loop

```

---

Algorithm 1 describe the process of one task *this\_task* being assigned to one of the UAV nodes or server according to decision parameters  $[x^m(\tau), x^s(\tau)]$  with the current time-slot. Assuming that the user who sends *this\_task* is  $u_i$ , we start by finding the nearest UAV node to ensure a stable connection. Line 9 judges if *this\_task* is  $\{1, 1\}$  or  $\{1, 0\}$ . That is, we aim at using UAV nodes at the edge as much as possible when computing resources are sufficient in the UML system.  $m_j.state$  stands for the work status indicator, 1 for occupied and 0 for idle. Time complexity of Algorithm 1 is  $O(n_{\tau})$ .

Second, to manage the FIFO task queue defined in Equation (26), we propose TQMS, as shown in Algorithm 2.

Follow the steps in Algorithm 1, when *this\_task* does not find an idle UAV node within this  $\tau$ , *this\_task* will be pushed into  $Q_t$  again to wait for the chance in next  $\tau$  (line9). Then as shown in line 12-17, we push the new tasks *newtask* into  $Q_t$  until reaching maximum capacity  $C_Q$ . In our design in UML, besides performing the tasks assigned by STAS, UAV nodes can receive nearby user requests containing GPS position information at any time. The time complexity is  $O(n_{\tau}(n_{task} + n_{newtask}))$ .

With the help of STAS and TQMS, we can manage the requests collected by UAV nodes, and select service provider for each of them considering the time & energy cost as well as the work state of nodes and server.

#### 5 SIMULATION AND ANALYSIS

Here we evaluate our proposed strategies by simulation experiments in achieving UAV-mounted mobile edge computing for disaster management.

As shown in TABLE 2, there exist 100 users in a square affected area  $\mathbb{R}^2$  after the disaster. We have 50 UAVs as carriers for providing MEC services to users in need. UAVs fly at

### Algorithm 2 TQMS: Task Queue Management Strategy

```

1: newtask // new tasks received within the current  $\tau$ 
2: loop
3:    $\tau = \tau + 1$ 
4:    $n\_task = Q_t.size$ 
5:   for  $i = 1$  to  $n\_task$  do
6:      $this\_task \leftarrow Q_t.pop()$ 
7:     task assignment
8:     if  $this\_task.x^m(\tau) = 1 \parallel this\_task.x^s(\tau) = 1$  then
9:        $Q_t.push(this\_task)$ 
10:    end if
11:  end for
12:  for  $i = 1$  to  $newtask.size$  do
13:    if  $Q_t.size < C_Q$  then
14:       $Q_t.push(newtask(i))$ 
15:    else
16:      break
17:    end if
18:  end for
19: end loop

```

TABLE 2  
Experimental settings

Parameter	Value	Parameter	Value
Number of users	100	$d_{fs}, d_0$	5, 100 m
Number of UAVs	50	$\gamma_{los}, \gamma_{nlos}$	2, 2.5
Flight altitude of UAVs	100 m	$X_g^{los}, X_g^{nlos}$	5, 20 dB
Bit rate of LoRa	50 kbps	$\alpha, \beta$	15.27, -0.88
Frequency of LoRa	1 GHz	$\gamma_{ld}$	2
Bandwidth of LoRa	500 kHz	$X_g^{ld}$	0 dB
Transmit Power of LoRa	100 mW	$\sigma_g^2$	-100 dBm
Battery Capacity	5700 mAh		

an altitude of 100 m and receive requests from user devices at any time. LoRa concentrator at the center of the area plays the role of collecting user requests and handing them over to the central server for task management and assignment. We set the carrier frequency, bandwidth and maximum transmit power of LoRa to 1 GHz, 500 kHz and 100 mW (20 dBm). We suppose that each UAV has a 5700 mAh battery (the large-capacity battery for DJI Matrice 100). Once a UAV becomes low on battery power, we need to recharge it before assigning any user request [1]. And for communication in the air-to-ground part, we use the parameters in 802.11n. We choose the suburban environment model [38] for  $\alpha$  and  $\beta$  used in calculating the probability of LoS/NLoS path loss.

In each  $\tau$ , devices in User Tier send requests to UAV nodes in the patrol model or passing by. With the help of long-range, low-cost LoRa connection, UAV nodes can forward requests up to concentrator immediately together with the work state information  $y^m(\tau)$ . Central server decides the task performers of each task in queue according to the users' locations  $\{\phi, \lambda, h\}$  and specific requirements  $x^m(\tau)$ . Central server also participates in task processing when  $x^s(\tau) = 1$ . At last, the tasks can not find idle UAV nodes, or available computational resources in the server will be pushed back into  $Q_t$  with new ones received in this  $\tau$ . We set different  $l_\tau$  from 100 ms to 500 ms and repeat each

group 10000 times. For better comparison, we have unified the simulation results by calculating the relative values in 1000 s.

The reason we choose  $l_\tau$  as a variable in performance evaluation is that, as we choose the Markov chain model to describe the system state transition, it is especially important when defining discrete time-slot. In the case that the other experiment settings are the same, the length of  $\tau$  may affect the overall state change frequency and also influence performance parameters such as latency under different conditions. Besides, if user density  $\rho_u$  changes in x-axis while the total number stays the same, we would like to explore what kind of increase in burden may be brought to UAVs in use, and how LoRa can enhance the UML system such as no excessive fluctuations in time or energy consumption.

Fig. 4 shows the total time cost of all 50 UAVs in the whole simulation. We separately consider the situation of three modes in Fig. 3. Here we use blue, red and yellow to distinguish different  $l_\tau$  100 ms, 200 ms and 500 ms, respectively. The lines with circle markers are our methods. Edgeless refers to a comparative experiment that under the same settings, UAVs only play the role of relay nodes. First, in Fig. 4a, time cost on UAV patrol mode shows that when UAV are waiting for service, there exists no difference between task management methods. Then for different  $l_\tau$ , time cost in this mode is consistent with  $l_\tau$  from high to low in numerical value. Yellow lines with  $l_\tau = 500$  ms is far higher than the other results. This can be explained that in our system model design, large  $l_\tau$  may reduce the system state transition speed. And in relation to the time spent on UAV patrolling, it is possible to perform multiple task assignments within the same time (such as flying to an area that has not been visited and then picking up new tasks), and only a few commands can be executed when  $l_\tau$  is large.

Second, in Fig. 4b which is different from Fig. 4a,  $t_{fly}$  refers to the time cost on UAV flying with purposes. As a result, considering that the rest time cost on UAV hovering and transmitting is relatively short, there should exist some inverse relationship between value in two subfigures. The results meet our expectations that when the user density decreases in the x-axis, all colored lines show a noticeable downtrend in Fig. 4a while lines are uptrend in Fig. 4b. Even for situation of different  $l_\tau$ . In Fig. 4b, blue lines with  $l_\tau = 100$  ms fly for the longest time while in Fig. 4a the complete opposite results appear. Here we can conclude that within the same experiment time, since we did not require the UAVs to fly faster in more sparse areas, and the total time cost of their actual movements is relatively kept within a numerical range.

Third, in Fig. 4c, the overall trend of time cost on UAV hovering to provide service is decreasing when user density increases. This can be explained that for the same experiment time, UAVs have to spend more time on moving among users and less on hovering to provide service. The differences between different task management methods start to appear. The results show that our method can reduce much of the time cost on UAV hovering while satisfying the same number of users.

To further evaluate the performance of our methods in emergency communication, we also calculate the results



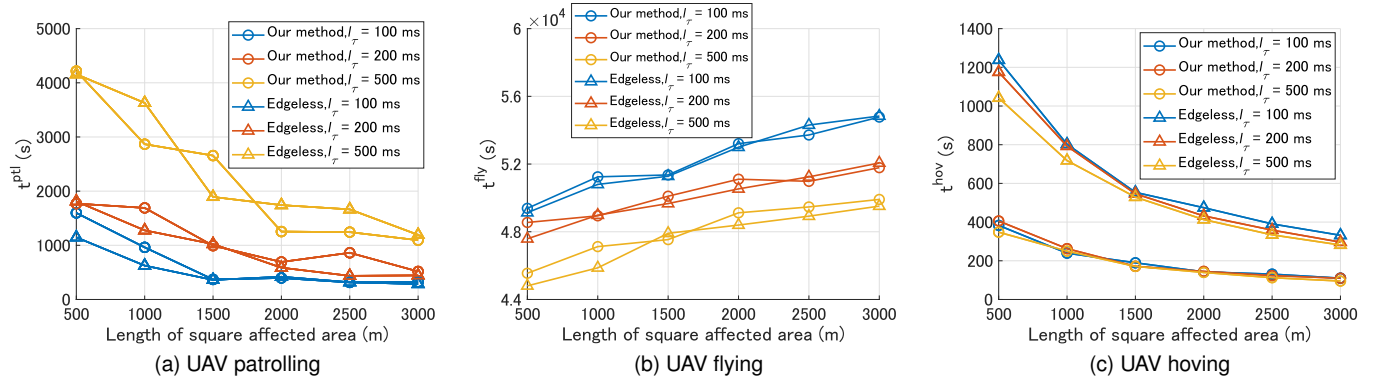


Fig. 4. Simulation results of time cost on UAV-based mobile edge computing using LoRaWAN.

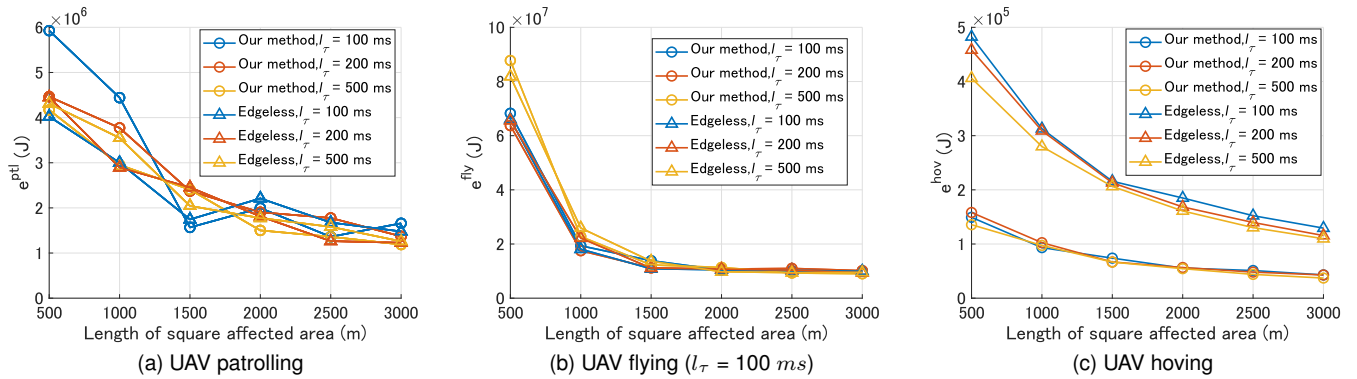


Fig. 5. Simulation results of time cost on UAV-based mobile edge computing using LoRaWAN.

of energy cost on three modes shown in Fig. 3. For UAV patrolling and flying, it seems that the results of different  $\tau$  or methods can not be easily distinguished from each other. We analyze that energy consumption on UAVs moving faces uncertainties from speed variation. This point also can be reflected in Fig. 5a and 5b that when a UAV has to move farther before providing service, the proportion of UAV flying at a constant speed will noticeably increase, which resulting in the reduction on energy cost. According to Equation (24), Fig. 5c shows the same trend as Fig. 4c.

Besides two main metrics, we also consider the path loss (dB), SNR (dB), and channel capacity (Mbit/s) of air-to-ground and remote-to-air communications.

Fig. 6 shows the path losses of the two parts. The path loss in LoS/NLoS model of air-to-ground communication stays at about 105.41 dB. And for the remote-to-air part in log-distance model of LoRaWAN, path loss increases with sparser user density. Both our method and Edgeless show similar results and trends, which means path loss may not be influenced by applying different strategies in task management.

Then in 7, the SNR of air-to-ground in LoS/NLoS model stays at 28.77 dB. And for the remote-to-air part in log-distance model of LoRaWAN, SNR shows a downtrend facing sparser user density.

Lastly, we calculate the channel capacity by Equations (11) and (14). The air-to-ground part in 802.11n has a larger channel capacity using our methods in task management. The green line with the circle marker shows the channel

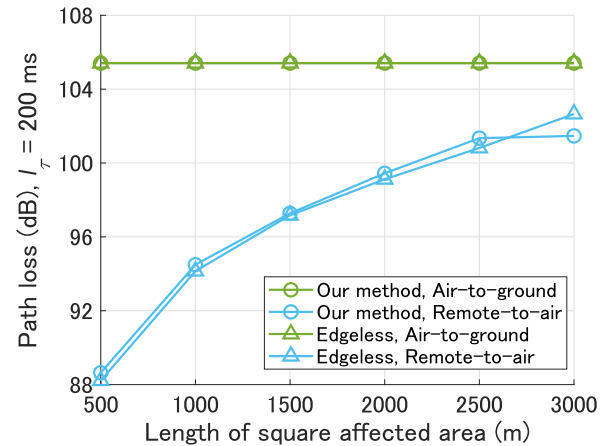


Fig. 6. Simulation results of path loss on UAV-based mobile edge computing using LoRaWAN.

capacity slightly fluctuates around 17 Mbit/s. The rest, green line with triangle marker, and light blue lines are lower than 4 Mbit/s. The overall results show that channel capacity does not change much with user density.

In summary, through the simulation results of time and energy cost, path loss, SNR, and channel capacity, our proposed task management strategies can provide low-cost MEC services based on UAV and LoRaWAN to users in the affected area after a disaster.

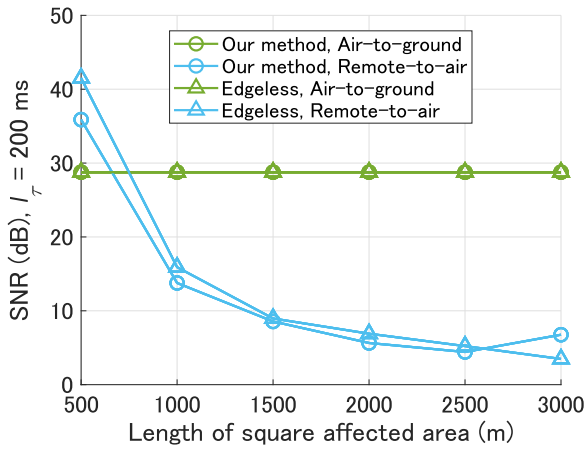


Fig. 7. Simulation results of SNR on UAV-based mobile edge computing using LoRaWAN.

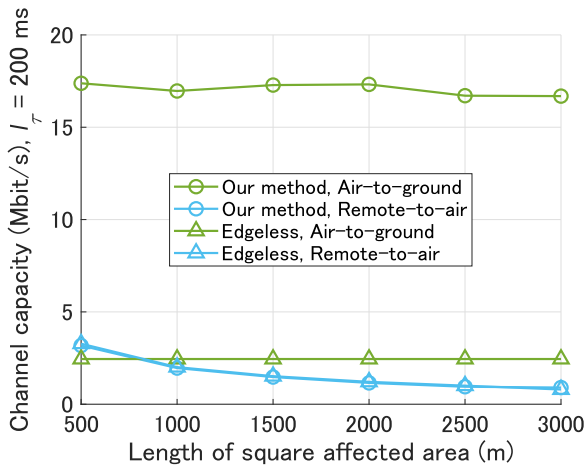


Fig. 8. Simulation results of channel capacity on UAV-based mobile edge computing using LoRaWAN.

## 6 CONCLUSION

In this paper, by studying the state-of-the-art technologies in recent years, we discover the potential to combine UAV technology and LoRaWAN communication into the implementation of MEC services for disaster management. We first propose a 3-tier network model including User Tier, UAV-mounted edge nodes as Service Tier, and LoRa concentrator & central server as Control Tier. We model the two parts in the UML system, air-to-ground and remote-to-air. We choose the LoS/NLoS path loss model for air-to-ground and log-distance for remote-to-air to describe the communication ways. We use the Markov chain to define the work state of Service Tier and Control Tier and propose two algorithms in solving task assignment and queue management. In performance evaluation, we choose time and energy cost, path loss, SNR, and channel capacity as metrics and consider the lengths of time-slot as well as user density in experimental settings. The results show that our solutions can achieve low-cost, long-range MEC services in disaster management based on UAVs and LoRaWAN.

The future work will include more technical details in network model design, and using UAVs such as DJI

Matrice 100 and Matrice 210 RTK V2 [1] to realize actual deployment. Our final target is to build a multi-UAV system to provide MEC and other communication services in contributing to disaster management.

## ACKNOWLEDGMENT

This work is partially supported by JSPS KAKENHI Grant Numbers JP19K20250, JP20F20080, JP20H04174 and Leading Initiative for Excellent Young Researchers (LEADER), MEXT, Japan. Mianxiong Dong is the corresponding author.

## REFERENCES

- [1] DJI, "DJI - the world leader in camera drones/quadcopters for aerial photography." [Online]. Available: <https://www.dji.com/>
- [2] M. Patel, B. Naughton, C. Chan, N. Sprecher, S. Abeta, A. Neal *et al.*, "Mobile-edge computing introductory technical white paper," *White Paper, Mobile-edge Computing (MEC) industry initiative*, 2014.
- [3] J. Xu, K. Ota, and M. Dong, "Fast networking for disaster recovery," *IEEE Transactions on Emerging Topics in Computing*, pp. 1–1, 2018.
- [4] V. Prajzler, "Lora, lorawan and loriot.io," 2015. [Online]. Available: <https://www.loriot.io/lorawan.html>
- [5] LoRa Alliance Technical Committee, "Lo-ran 1.1 specification," 2017. [Online]. Available: [https://lora-alliance.org/sites/default/files/2018-04/lorawantm\\_specification\\_v1.1.pdf](https://lora-alliance.org/sites/default/files/2018-04/lorawantm_specification_v1.1.pdf)
- [6] M. Mozaffari, W. Saad, M. Bennis, and M. Debbah, "Communications and control for wireless drone-based antenna array," *IEEE Transactions on Communications*, pp. 1–1, 2018.
- [7] N. H. Motlagh, M. Bagaa, and T. Taleb, "Uav-based iot platform: A crowd surveillance use case," *IEEE Communications Magazine*, vol. 55, no. 2, pp. 128–134, February 2017.
- [8] M. Dong, K. Ota, L. T. Yang, A. Liu, and M. Guo, "Lscd: A low-storage clone detection protocol for cyber-physical systems," *IEEE Transactions on Computer-Aided Design of Integrated Circuits and Systems*, vol. 35, no. 5, pp. 712–723, May 2016.
- [9] S. Sekander, H. Tabassum, and E. Hossain, "Multi-tier drone architecture for 5g/b5g cellular networks: Challenges, trends, and prospects," *IEEE Communications Magazine*, vol. 56, no. 3, pp. 96–103, March 2018.
- [10] A. Al-Hourani and K. Gomez, "Modeling cellular-to-uav path-loss for suburban environments," *IEEE Wireless Communications Letters*, vol. 7, no. 1, pp. 82–85, February 2018.
- [11] Z. Hu, Z. Zheng, L. Song, T. Wang, and X. Li, "Uav offloading: Spectrum trading contract design for uav-assisted cellular networks," *IEEE Transactions on Wireless Communications*, vol. 17, no. 9, pp. 6093–6107, September 2018.
- [12] World Confederation for Physical Therapy, "What is disaster management?" 2016. [Online]. Available: <https://www.wcpt.org/disaster-management/what-is-disaster-management>
- [13] M. Erdelj, E. Natalizio, K. R. Chowdhury, and I. F. Akyildiz, "Help from the sky: Leveraging uavs for disaster management," *IEEE Pervasive Computing*, vol. 16, no. 1, pp. 24–32, January 2017.
- [14] K. Ota, M. Dong, J. Gui, and A. Liu, "Quoin: Incentive mechanisms for crowd sensing networks," *IEEE Network*, vol. 32, no. 2, pp. 114–119, March 2018.
- [15] S. A. R. Naqvi, S. A. Hassan, H. Pervaiz, and Q. Ni, "Drone-aided communication as a key enabler for 5g and resilient public safety networks," *IEEE Communications Magazine*, vol. 56, no. 1, pp. 36–42, January 2018.
- [16] S. Sardellitti, G. Scutari, and S. Barbarossa, "Joint optimization of radio and computational resources for multicell mobile-edge computing," *IEEE Transactions on Signal and Information Processing over Networks*, vol. 1, no. 2, pp. 89–103, June 2015.
- [17] C. You, K. Huang, H. Chae, and B. Kim, "Energy-efficient resource allocation for mobile-edge computation offloading," *IEEE Transactions on Wireless Communications*, vol. 16, no. 3, pp. 1397–1411, March 2017.

- [18] X. Tao, K. Ota, M. Dong, H. Qi, and K. Li, "Performance guaranteed computation offloading for mobile-edge cloud computing," *IEEE Wireless Communications Letters*, vol. 6, no. 6, pp. 774–777, December 2017.
- [19] S. Jeong, O. Simeone, and J. Kang, "Mobile edge computing via a uav-mounted cloudlet: Optimization of bit allocation and path planning," *IEEE Transactions on Vehicular Technology*, vol. 67, no. 3, pp. 2049–2063, March 2018.
- [20] J. Wu, M. Dong, K. Ota, J. Li, and Z. Guan, "Fcsc: Fog computing based content-aware filtering for security services in information centric social networks," *IEEE Transactions on Emerging Topics in Computing*, pp. 1–1, 2018.
- [21] J. Wu, M. Dong, K. Ota, J. Li, W. Yang, and M. Wang, "Fog-computing-enabled cognitive network function virtualization for an information-centric future internet," *IEEE Communications Magazine*, vol. 57, no. 7, pp. 48–54, 2019.
- [22] H. Li, K. Ota, and M. Dong, "Eccn: Orchestration of edge-centric computing and content-centric networking in the 5g radio access network," *IEEE Wireless Communications*, vol. 25, no. 3, pp. 88–93, June 2018.
- [23] —, "Deep reinforcement scheduling for mobile crowdsensing in fog computing," *ACM Transactions on Internet Technology (TOIT)*, vol. 19, no. 2, pp. 1–18, 2019.
- [24] J. Petajajarvi, K. Mikhaylov, A. Roivainen, T. Hanninen, and M. Pettissalo, "On the coverage of lpwans: range evaluation and channel attenuation model for lora technology," in *2015 14th International Conference on ITS Telecommunications (ITST)*, December 2015, pp. 55–59.
- [25] M. C. Bor, U. Roedig, T. Voigt, and J. M. Alonso, "Do lora low-power wide-area networks scale?" in *Proceedings of the 19th ACM International Conference on Modeling, Analysis and Simulation of Wireless and Mobile Systems*, ser. MSWiM '16. New York, NY, USA: ACM, 2016, pp. 59–67. [Online]. Available: <http://doi.acm.org/10.1145/2988287.2989163>
- [26] M. Rizzi, P. Ferrari, A. Flammini, and E. Sisinni, "Evaluation of the iot lorawan solution for distributed measurement applications," *IEEE Transactions on Instrumentation and Measurement*, vol. 66, no. 12, pp. 3340–3349, December 2017.
- [27] O. Georgiou and U. Raza, "Low power wide area network analysis: Can lora scale?" *IEEE Wireless Communications Letters*, vol. 6, no. 2, pp. 162–165, April 2017.
- [28] F. Adelantado, X. Vilajosana, P. Tuset-Peiro, B. Martinez, J. Melia-Segui, and T. Watteyne, "Understanding the limits of lorawan," *IEEE Communications Magazine*, vol. 55, no. 9, pp. 34–40, September 2017.
- [29] F. Baccelli and B. Blaszczyszyn, "Stochastic geometry and wireless networks: Volume ii applications," *Foundations and Trends in Networking*, vol. 4, no. 1-2, pp. 1–312, 2010. [Online]. Available: <http://dx.doi.org/10.1561/13000000026>
- [30] M. Chen, M. Mozaffari, W. Saad, C. Yin, M. Debbah, and C. S. Hong, "Caching in the sky: Proactive deployment of cache-enabled unmanned aerial vehicles for optimized quality-of-experience," *IEEE Journal on Selected Areas in Communications*, vol. 35, no. 5, pp. 1046–1061, May 2017.
- [31] A. Al-Hourani, S. Kandeepan, and S. Lardner, "Optimal lap altitude for maximum coverage," *IEEE Wireless Communications Letters*, vol. 3, no. 6, pp. 569–572, December 2014.
- [32] RAK, "Lora module rak811." [Online]. Available: <https://www.rakwireless.com/en/module/lora/RAK811>
- [33] G. J. Leishman, *Principles of helicopter aerodynamics with CD extra*. Cambridge university press, 2006.
- [34] Y. Zeng and R. Zhang, "Energy-efficient uav communication with trajectory optimization," *IEEE Transactions on Wireless Communications*, vol. 16, no. 6, pp. 3747–3760, June 2017.
- [35] C. D. Franco and G. Buttazzo, "Energy-aware coverage path planning of uavs," in *2015 IEEE International Conference on Autonomous Robot Systems and Competitions*, April 2015, pp. 111–117.
- [36] J. Liu, Y. Mao, J. Zhang, and K. B. Letaief, "Delay-optimal computation task scheduling for mobile-edge computing systems," in *2016 IEEE International Symposium on Information Theory (ISIT)*, July 2016, pp. 1451–1455.
- [37] L. Wan, W. Lou, E. Abner, and R. J. Kryscio, "A comparison of time-homogeneous markov chain and markov process multi-state models," *Communications in Statistics: Case Studies, Data Analysis and Applications*, vol. 2, no. 3-4, pp. 92–100, 2016. [Online]. Available: <https://doi.org/10.1080/23737484.2017.1361366>

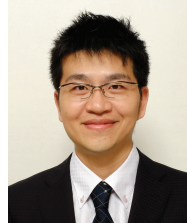
- [38] J. Holis and P. Pechac, "Elevation dependent shadowing model for mobile communications via high altitude platforms in built-up areas," *IEEE Transactions on Antennas and Propagation*, vol. 56, no. 4, pp. 1078–1084, April 2008.



**Jianwen Xu** received the B.Eng degree in Electronic and Information Engineering from Dalian University of Technology in 2014, M.Eng degree in Information and Communication Engineering from Shanghai Jiao Tong University in 2017, and Ph.D. degree in Engineering from Muroran Institute of Technology in 2020. He is currently a postdoctoral researcher at Muroran Institute of Technology. He receives the JSPS Postdoctoral Fellowship for Research in Japan for 2020 Fiscal Year. He was selected as a Non-Japanese Researcher by NEC C&C Foundation for 2019 Fiscal Year. His main fields of research interest include edge computing, Internet of things.



**Kaoru Ota** was born in Aizu-Wakamatsu, Japan. She received M.S. degree in Computer Science from Oklahoma State University, the USA in 2008, B.S. and Ph.D. degrees in Computer Science and Engineering from The University of Aizu, Japan in 2006, 2012, respectively. Kaoru is currently an Associate Professor and Ministry of Education, Culture, Sports, Science and Technology (MEXT) Excellent Young Researcher with the Department of Sciences and Informatics, Muroran Institute of Technology, Japan. From March 2010 to March 2011, she was a visiting scholar at the University of Waterloo, Canada. Also, she was a Japan Society of the Promotion of Science (JSPS) research fellow at Tohoku University, Japan from April 2012 to April 2013. Kaoru is the recipient of IEEE TCSC Early Career Award 2017, and The 13th IEEE ComSoc Asia-Pacific Young Researcher Award 2018. She is Clarivate Analytics 2019 Highly Cited Researcher (Web of Science).



**Mianxiong Dong** received B.S., M.S. and Ph.D. in Computer Science and Engineering from The University of Aizu, Japan. He is the Vice President and youngest ever Professor of Muroran Institute of Technology, Japan. He was a JSPS Research Fellow with School of Computer Science and Engineering, The University of Aizu, Japan and was a visiting scholar with BBCC group at the University of Waterloo, Canada supported by JSPS Excellent Young Researcher Overseas Visit Program from April 2010 to August 2011. Dr. Dong was selected as a Foreigner Research Fellow (a total of 3 recipients all over Japan) by NEC C&C Foundation in 2011. He is the recipient of IEEE TCSC Early Career Award 2016, IEEE SCSTC Outstanding Young Researcher Award 2017, The 12th IEEE ComSoc Asia-Pacific Young Researcher Award 2017, Funai Research Award 2018 and NISTEP Researcher 2018 (one of only 11 people in Japan) in recognition of significant contributions in science and technology. He is Clarivate Analytics 2019 Highly Cited Researcher (Web of Science).